Food Packaging and Shelf Life 26 (2020) 100564

Contents lists available at ScienceDirect

Food Packaging and Shelf Life

journal homepage: www.elsevier.com/locate/fpsl

Potential of Silver-Kaolin in Gelatin Composite Films as Active Food Packaging Materials

I.S. Nur Amila Najwa [a], M. Mat Yusoff [a], Z.A. Nur Hanani [a,b,*]

[a] Department of Food Technology, Faculty of Food Science and Technology, Universiti Putra Malaysia, 43400, UPM, Serdang, Selangor, Malaysia
[b] Halal Products Research Institute, Universiti Putra Malaysia, 43400, UPM, Serdang, Selangor, Malaysia

ARTICLE INFO

Keywords:
Biodegradable films
active packaging
fish gelatin
kaolin
silver

ABSTRACT

This study discovered the potential application of kaolin (Kln) and silver-kaolin (Ag-Kln) in gelatin-composite films as active packaging material for food products. Three different types of kaolins; raw Kln, Ag-Kln (1:2) mix and Ag-Kln (1:1) mix with various concentrations (15%, 30% and 45%) were prepared by solution casting. For the water barrier properties, the wettability test indicated that the addition of kaolin in gelatin films produced hydrophobic films and lower ($p < 0.05$) water vapour permeability, regardless of the kaolin type and concentration. Scanning electron microscopy images portrayed that higher inclusions of Ag-Kln compounds are able to develop smoother surface and homogenous cross-section. In addition, by incorporating these two materials, films with great antimicrobial effect towards both Gram-positive and Gram-negative bacteria were produced. Elevation of Ag-Kln concentration also proved to lower the transmission of ultraviolet-vis light through the films. These findings suggested that gelatin film with Ag-Kln has a potential and beneficial in food packaging industry due to its enhanced properties.

1. Introduction

Demand for foods in the next 30-40 years is expected to grow rapidly due to progression in human population, increasing consumer purchasing power and urbanization (Satterthwaite, McGranahan, & Tacoli, 2010). Producers and stakeholders need to make a significant investment in producing more environmentally sustainable products in the future. Advanced packaging has a distinctive role in enhancing food security, reducing food losses and prolonging the shelf life. Nowadays, research on active packaging has evolved tremendously due to its potential in delaying food spoilage and extending the shelf life of food products.

Active packaging reinforced with natural extracts has been emphasized due to the safety concerns and consumer's preference (Jridi et al., 2019). Bio-polymer packaging helps in conserving the environment while protecting the food by improving the barrier towards oxidative agent, external moisture and aroma. Natural bio-composite films are usually made from proteins, polysaccharides, and lipids. Their great characteristics are not limited to sustainability and eco-friendly, they also edible, biodegradable, and safe for human consumption (Li, Yang, Deng, Guo, & Xue, 2020). Gelatin is an abundance protein-based biodegradable component derived from the hydrolysis process of animals' collagen (Liu et al., 2020). Kam et al. (2018) reported that gelatin possesses numerous properties, for instance, as thickening agent and stabilizer. Gelatin's characteristics depend on the versatility (different sources) and various features subjected to the ages of animals, processes, etc.

Fish gelatin films exhibit lower water vapour permeability and relatively low moisture stability due to the variances in amino acid composition. It is also suggested to incorporate other fillers to fabricate bio-composite films with better applicability (Hosseini & Gómez-Guillén, 2018). Liu et al. (2020) stated that films with high-resistance and flexibility were produced due to the reaction occurred which affected the crosslink network physically. Studies using gelatin as the polymer base had shown better properties, including great barrier against ultra-violet (UV) light, gases, volatile substances, and thermal (Li et al., 2020; Liu et al., 2020) owing to its innate chemical structure (Abedinia, Ariffin, Huda, & Nafchi, 2018). Several studies revealed that composite films can be formulated to improve water and gas barrier properties (Al-Hassan & Norziah, 2012; Suderman, Isa, & Sarbon, 2018). Blending gelatin with other biopolymers not only reduces the hydrophilicity, it may also recover both the physical and

* Corresponding author at: Department of Food Technology, Faculty of Food Science and Technology, Universiti Putra Malaysia, 43400, UPM, Serdang, Selangor, Malaysia.
E-mail address: Hanani@upm.edu.my (Z.A. Nur Hanani).

https://doi.org/10.1016/j.fpsl.2020.100564
Received 10 February 2020; Received in revised form 7 July 2020; Accepted 27 August 2020
Available online 17 September 2020

functional properties of films (Ghaderi, Hosseini, Keyvani, & Gómez-Guillén, 2019; Córdoba & Sobral, 2017).

Kaolin was formerly used in the paper industry due to its economical-friendliness and sustainability (Maisanaba et al., 2015). It is a hydrated aluminosilicate with a soft structure and exists as a white clay mineral that belongs to a part of the group of industrial minerals (Maisanaba et al., 2015). Kaolin is applied as paper coating to improve the brightness, smoothness and glossiness (Bergaya & Lagaly, 2013). It also enhances printability of the paper (Ma & Bruckard, 2010). Kaolin is also being used in tableware and ceramics (Mecif, Soro, Harabi, & Bonnet, 2010) for its hardness and colour attributes.

According to Food and Drugs Administration (Food & Drug Administration, 2002), kaolin is listed with the other minerals substances that are considered as "Generally Recognized As Safe" (GRAS) when added indirectly to human food with no limitation. It also has been used in the manufacturing of paper and paperboard which contacts with food. Kaolin which is used as an extra filler in the gelatin film matrix is predicted to increase the tortuosity of permeant molecules diffusion path. Kaolinite particles possess di-octahedral minerals within the chain structure, bonded with a single layer of silica tetrahedral layer (SiO_4) and a layer of aluminium octahedral (Al_2 $(OH)_4$). This explanation clarifies the compound's ability in blocking the water penetration. These bonded layers consist of embedded oxygen anion between Al and Si, which are also known as platelets. The platelets give no response when hydrated due to the strong hydrogen bonding (Slivka, 2002), which in turn, produces a better hygroscopic material. On the other hand, kaolin is a good carrier for silver in optimizing the antimicrobial activity towards both Gram-negative and Gram-positive foodborne pathogens.

Silver in kaolin clay is found to be useful since it helps in enhancing the antibacterial activities of kaolin (Jou & Malek, 2016). Silver has been recognized as a good additional active ingredient to blend with natural polymers, such as gelatin, starch, chitosan and cellulose in producing food packaging materials, due to its potential in antibacterial activity, good thermal stability and low toxicity (Qin, Liu, Yuan, Yong, & Liu, 2019). Roy, Shankar, and Rhim (2019) and Salari, Khiabani, Mokarram, Ghanbarzadeh, and Kafil (2018) revealed that silver was not just succeeded in inhibiting pathogens growth, but also increased the mechanical strength of polysaccharide-based films. Research by Sharma, Yngard, and Lin (2009) claimed that silver particles in a small consumption gave advantageous effects towards human being's health. Silver has been included in developing antibiotic for human consumption in the medical field for bacteria resistance (Odeniyi, Okumah, Adebayo-Tayo, & Odeniyi, 2020) due to its effectiveness in antimicrobial activity, chemical stability, and excellent catalytic effect (Kumar, Pammi, Kollu, Satyanarayana, & Shameem, 2014). Rao et al. (2019) explored that silver employed in antibiotics had great potential as an anti-cancer, with its capability in fungicide and bactericide. However, there is a concern about the safety of silver in the application of food packaging materials. According to European Food Safety Authority (EFSA Panel on food contact materials, enzymes, flavourings & processing aids (CEF), 2011), silver ion migration rate from the packaging film matrix to its contents is limited up to 0.05 mg Ag/kg food.

To the best of our knowledge, there has been no ample research on the application of kaolin in gelatin-based films and the combination of kaolin as fillers with silver compound for active packaging materials. Therefore, this study was carried out to develop gelatin composite films reinforced with silver-kaolin as an active packaging material.

2. Materials and Methods

2.1. Chemicals

Fish gelatin used was 240-260 Bloom, supplied from Custom Collagen (Addison, Illinois, USA). Kaolin (Kln) and silver kaolin (Ag-Kln) was bought from Provet Group of Companies, Selangor, Malaysia. Buffered peptone water, nutrient agar and nutrient broth were obtained from EMD Millipore Corporation (Billerica MA, USA). Mueller-Hinton agar was purchased from Merck Sdn. Bhd. (Selangor, Malaysia) whereas, glycerol (99.5% purity) was supplied from Systerm (Karlsruhe, Germany). *Staphylococcus aureus* (ATC 12600), *Listeria monocytogenes* (ATCC 19111), *Salmonella typhimurium* (ATCC 13311), and *Escherichia coli* (ATCC 11229) were obtained from microbiology lab, Universiti Putra Malaysia.

2.2. Film Preparation

Gelatin powder, 4 g was dissolved in 70 °C distilled water for 30 min as described by Tongnuanchan et al. (2015). Then, 12.5% (w/w) glycerol as a plasticizer was added in the film-forming solution (FFS) in the range of 45-50 °C. Next, different kaolin powder; raw kaolin, Ag-Kln (1:2) mix and Ag-Kln (1:1) mix were added with 15%, 30%, and 45% concentrations. Ag-Kln (1:2) mix represents the ratio of 1:2 of silver particles to kaolin amount, whereas Ag-Kln (1:1) mix represents a 1:1 ratio of silver to kaolin. Again, the temperature was increased to 70 °C and the solution was stirred well. Mixing was done for 30 min on a hot plate. Twenty mL of FFS was poured on plastic petri dishes (64 cm^2) and dried at 28 °C for 48 h before peeling. Finally, the dry films were conditioned at 23 ± 2 °C with relative humidity (RH) of 50 ± 5% prior to analysis. A film without kaolin and Ag-Kln was prepared as a control.

2.3. Film Thickness

The thickness of the film was measured by using a digital micrometre (Mitutoyo Co., Kawasaki, Japan). Different spots were tested, including the centre of the film for both thickness and mechanical test. A total of six measurements were calculated to obtain the films' average thickness.

2.4. Opacity

The opacity test was carried out according to the procedure by Maryam Adilah, Jamilah, & Nur Hanani, 2018. The films were cut into rectangular size (1 × 4 cm) to be fit inside the cuvette of Genesys 20 UV-Vis spectrophotometer (Thermo Fisher Scientific, Madison, Wisconsin, USA). Absorbance measurement of each film was recorded at 600 nm, and calculation for the opacity was as below:

$$\text{Opacity} = \text{Abs}_{600}/\text{x}$$

where Abs_{600} is the absorbance value at 600 nm and x was the thickness of the film (mm).

2.5. Mechanical Properties

Tensile strength (TS), Young's modulus (YM) and elongation at break (EAB) of the films were assessed by using INSTRON 3365 Machine (Instron Co., Canton, Massachusetts, USA). Eight measurements on average were evaluated, with each film cut into 1.5 cm wide and 9 cm long. Films were then conditioned at 23 ± 2 °C and RH of 50 ± 5% for 48 hours before further analysis. The strips were gripped before the machine started to stretch the films at 50 mm/min of crosshead speed and 10 kN of tensile load. Five cm was set for the initial separation. The tensile strength (σ = force/initial cross-sectional area), elongation at break (E) and Young's modulus (EM) values were obtained from the Instron Bluehill Universal Software (Norwood, MA, USA).

2.6. Scanning Electron Microscopy (SEM)

The scanning electron microscopy (SEM), model LEO 1455 SPEM (Cambridge, United Kingdom) was used to view the surfaces and cross-section structures of the films. Firstly, samples were fixed on bronze stub and carbon-taped before sputtered coated with gold and vacuumed using Sputter Coater SCD 005 (BAL-TEC SCD) for 20 min. Visualizing

analysis was done using magnification ranging from 250 to 3000x with accelerating voltage at 12-15 kV.

2.7. Atomic Force Microscopy (AFM)

The roughness of the film was determined using Dimension Edge atomic force microscope (Bruker Crest, Camarillo, California, USA). The analysis mode was set up using ScanASYST (Peak force Tapping Mode) and SCANASYST-AIR cantilever (T =650 nm, L = 115 μm, W = 25 μm, f_o =70 kHz, k =0.4 N/m). The scan size used was 8 x 8 μm at 5.0 μm/sec of scan rate. The root-mean-square roughness (Rq) was calculated and reported as the roughness value with an average of four replicates.

2.8. Ultra-Violet Light Transmission

Each film sample was analysed in triplicate for ultra-violet (UV) ray between 180 and 800 nm. Namely, there were 3 types of UV radiation that had been tested; UVA (320-400 nm), UVB (280-320 nm) and UVC (180-280 nm). Visible light wavelengths, ranging from 400-800 nm were also tested for all types of films. Films were cut into 1 × 4 cm size before placed in a cuvette. Empty cuvette was used as blank reference and absorbance was measured by using a UV-vis spectrophotometer (Thermo Fisher Scientific, Madison, Wisconsin, USA).

2.9. Water Solubility

A total of three films for each of the different types of samples were cut into a square (4 × 4 cm) and dried at 100 °C in a crucible for 24 h to determine the initial dry mass (Kavoosi, Rahmatollahi, Dadfar, & Purfard, 2014). Next, the films were immersed in 50 mL of distilled water and left for 24 h at room temperature. Then, the films were filtered through Whatman No. 1 filter paper and dried again in the oven at 100 °C for 24 h to determine the final dry mass. The equation below was used to calculate the water solubility (WS) of the films:

$$WS\ (\%) = [(W_0 - W_f) / W_0] \times 100$$

where W_o and W_f are initial and final dry mass, respectively.

2.10. Water Vapour Permeability (WVP)

The water vapour permeability (WVP) of the film sample was measured according to Maryam Adilah, Jamilah, & Nur Hanani, 2018. Crucibles were first filled with 6 mL of distilled water. Each film sample was then covered the top of the crucibles. Then, the crucibles were placed inside a desiccator that was tighten using seal grease. The temperature and RH were maintained at 25 ± 1 °C and 50 ± 2%, respectively. The temperature and RH were chosen due to the ASTM E96 WVP standard method with a slight modification.

The crucibles were weighed every hour for nine hours total interval, and a linear graph of weight gain versus time was performed. Four replicates were used for this analysis. The equation below was used to calculate the WVP of the film:

WVP = (weight difference) x (film thickness) / {(Exposed area) x (time) x (partial pressure difference)}

2.11. Moisture Content

The moisture content (MC) was measured according to the method of Soradech, Nunthanid, Limmatvapirat, and Luangtana-Anan (2012) with some modifications. The film samples were cut into 4 × 4 cm and left conditioned in a desiccator (RH = 50% ± 3% at 23 ± 2% °C) for 48 hours before analysis. Each film sample was then dried in an oven at 100 °C for 24 h. The weight before drying and the weight loss after drying were measured and expressed as a percentage, based on the final weight of the film. Four replicates were done per formulation.

2.12. Water Contact Angle

The water contact angle (WCA) was measured according to Garrido, Leceta, de la Caba, and Guerrero (2018) using contact angle metre, model OCA 15EC (Data Physics Instruments GmBH, Filderstadt, Germany). The film was cut into 3 cm x 10 cm strips and fixed on top of a glass slide. Then, the glass slide was placed on the movable stage attached to the contact angle analyzer and adjusted accordingly. Next, 3 μL of distilled water was dropped from 1.5 cm height on the sample's surface using a micro syringe. A camera that was set in the instrument was used to capture the image of both sides of the water droplet angles formed on the film's surface. The contact angles of the water droplet on both sides were computed using SCA20 software with five replicates for each film sample and averaged.

2.13. Antimicrobial Activity (Disc Diffusion Method)

The disc diffusion method (DDM) was used to assess the antimicrobial activity of the films (control, kaolin, and Ag-Kln) against food-borne pathogens (Ponce, Roura, del Valle, & Moreira, 2008). Discs with 5 mm were cut and tested against Gram-negative bacteria (*Escherichia coli (E. coli)* and *Salmonella typhimurium (S. typhimurium)*) and other two types of Gram-positive bacteria (*Staphylococcus aureus (S. aureus)* and *Listeria monocytogenes (L. monocytogenes)*). The bacteria were inoculated from the stock and dipped in the nutrient broth for growth. They were placed in an incubator shaker at 35 °C for 48 h before each of the bacteria was streaked on the nutrient agar plates and left for the next 24 h. Subsequently, discs which were sterilized beforehand were placed onto Mueller-Hinton agar which had been swabbed with the bacteria (approximately 10^6-10^7 CFU/mL of the tested bacteria). Then, they were left incubated inverted at 35 °C overnight and diameter of the inhibition zone halo was measured in mm to evaluate the antibacterial capacity of the films. All of the equipment and apparatus, including the films used in preparing the analysis were sterilized using autoclave for 30 min at 120 °C (Bauer, 1966; Gómez-Estaca, De Lacey, López-Caballero, Gómez-Guillén, & Montero, 2010).

2.14. Statistical Analysis

The statistical analysis was done using two-way (un-stacked) analysis of variance (ANOVA) and Tukey's multiple tests using Minitab 18 software (Minitab Inc., State College, Pennsylvania, USA) with significant level at ($p < 0.05$).

3. Results and Discussions

3.1. Physical Properties of Films

3.1.1. Film Thickness

This study revealed that the incorporation of raw kaolin in gelatin composite films resulted in a great increment of the thickness (Table 1). The differences were also significant between control, raw kaolin and Ag-Kln films. This might be due to the elevation of kaolin powder compound and silver particles which are presented within the polymer matrix. In another way, when comparing among different concentrations; 15%, 30%, and 45%, the differences observed were also significant. This could be due to the combined effect of kaolin, which incorporated between the protein network, as well as the increased solid content in the resulting films as supported by Jafarzadeh, Alias, Ariffin, Mahmud, and Najafi (2016) using semolina films reinforced with nanokaolin. This is also proved by the images obtained from SEM analysis in Fig. 1. A higher concentration of kaolin and silver-kaolin in gelatin films showed a significant effect on the thickness of the films caused by the greater amount of compounds introduced, which had interrupted the organized structure of the film matrix, thus resulted in a thicker film (Tongnuanchan, Benjakul, Prodpran, & Nilsuwan, 2015).

Table 1
Film thickness, opacity and mechanical properties of control gelatin film and gelatin films incorporated with raw kaolin, Ag-Kln (1:2) mix, and Ag-Kln (1:1) mix.

Film Samples	Concentration (%)	Thickness (μm)	Opacity	Young's Modulus (MPa)	Tensile strength (MPa)	Elongation at break (%)
Control	-	61.00 ± 1.00^{Cd}	0.08 ± 0.01^{Cd}	775.40 ± 17.50^{Aa}	18.20 ± 1.50^{Aa}	14.49 ± 0.45^{Abc}
Raw Kaolin	15%	75.00 ± 1.00^{Bc}	0.37 ± 0.02^{Bc}	42.36 ± 1.91^{Cc}	1.79 ± 0.06^{Bc}	17.18 ± 1.20^{Aa}
	30%	76.00 ± 3.00^{Bc}	0.52 ± 0.01^{Bb}	86.14 ± 3.16^{Cc}	1.85 ± 0.06^{Bc}	14.65 ± 0.52^{Ab}
	45%	80.00 ± 1.00^{Bc}	0.55 ± 0.01^{Ba}	114.17 ± 1.11^{Cb}	3.37 ± 0.06^{Bb}	12.48 ± 0.84^{Ac}
Ag-Kln (1:2) mix	15%	77.00 ± 2.00^{Ab}	0.74 ± 0.01^{Bc}	63.35 ± 8.34^{Cc}	1.76 ± 0.25^{Bc}	10.97 ± 0.84^{Ba}
	30%	81.00 ± 5.77^{Ab}	0.80 ± 0.05^{Bb}	121.32 ± 4.67^{Cc}	2.35 ± 0.15^{Bc}	8.65 ± 0.28^{Bb}
	45%	83.00 ± 2.65^{Ab}	1.31 ± 0.04^{Ba}	115.46 ± 16.15^{Cb}	2.38 ± 0.01^{Bb}	7.36 ± 1.69^{Bc}
Ag-Kln (1:1) mix	15%	76.00 ± 3.00^{Aa}	1.34 ± 0.01^{Ac}	63.50 ± 18.50^{Bc}	2.10 ± 0.06^{Bc}	14.67 ± 0.17^{Ba}
	30%	81.00 ± 1.50^{Aa}	1.42 ± 0.05^{Ab}	128.30 ± 7.68^{Bc}	2.61 ± 0.25^{Bc}	10.71 ± 0.57^{Bb}
	45%	89.00 ± 1.00^{Aa}	1.87 ± 0.02^{Aa}	376.20 ± 22.10^{Bb}	3.51 ± 0.18^{Bb}	4.32 ± 0.90^{Bc}

Values are given as mean ± standard deviation.
Small letters (a,b,c,d) in the same column indicate significant difference between concentrations ($p < 0.05$).
Capital letters (A,B,C) in the same column indicate significant difference between type of kaolin ($p < 0.05$).

Also, this result correlates to the increment of films' opacity values (Table 1).

3.1.2. Opacity

Optical properties are considered crucial especially in food packaging production as they can affect the consumers' acceptability of the food product. Raw kaolin film resulted in significant opacity increment than clear gelatin control film due to the addition of kaolin powder in the FFS. Physically, control film appearance was transparent whereas raw kaolin film was misty and cloudy. Control film also showed the lowest opacity value compared to the films added with kaolin and silver powder (Table 1). The tortuosity features of kaolin make it more suitable to be blended in aqueous solution compared to halloysite (Lee & Kim, 2002) and other clay; montmorillonite (Murray, 2000). Thus, developed film with greater opacity value, correlated to its advantageous attributes; low viscosity, good solubility and liquidity (Christidis, 2013; Okada, Yoshizaki, Kameshima, Nakajima, & MacKenzie, 2010), as well as good chemical stability (Cheng, Ye, Chang, & Wu, 2019; Hu, Wu, Xu, & Chen, 2018). The films' opacity increased ($p < 0.05$) gradually, proportional to the kaolin concentration, caused by the aggregation of increasing kaolin amount in gelatin polymer matrix. The distribution pattern of interaction between kaolin and gelatin can be observed from SEM image (Fig. 1c) which shows the accumulation of kaolin compounds on the film's surface. As silver particles were introduced into the solution, the opaqueness elevated ($p < 0.05$) explaining the increase in value and how it affected the UV-light transmission rate (Table 2).

An intense colour was observed for the FFS with the presence of silver and kaolin. This is due to the white metallic lustre of silver compounds causing the pure clear gelatin film to be more opaque and produced films with better organoleptic properties (Austin, 2007). Obvious significant differences were noticed among control film and films incorporated with kaolin and silver-kaolin. Ascribing to the increased in concentration, films with higher opacity level were developed. This was implied to the increase of impurities and yellowish colour of the films as a greater amount of Kln and Ag-Kln were added. The active compounds' colour gave resistance for the spectrophotometer to measure the films since more solid compounds were reinforced which justify the rise in value. According to Atarés, Bonilla, and Chiralt (2010), and Mbey, Hoppe, and Thomas (2012), the addition of concentration affected some colour parameters depending on the type of compound used.

3.1.3. Mechanical Properties

The strength of the film was determined based on the films' brittleness and elasticity. The mechanical properties should be able to protect the integrity of the packaged product (Yang et al., 2016). Young's modulus (YM) is a measure of the ability of a material to withstand changes in length when tension or compression is applied. Table 1 shows that YM values of the films decreased as kaolin was incorporated. However, the values then increased significantly ($p < 0.05$) proportional to the kaolin and silver content.

Control film was found to be more elastic than kaolin and Ag-Kln films. Nevertheless, among the films with active compounds; kaolin and Ag-Kln, the YM values were observed to increase significantly, which showed that incorporation of Ag-Kln (1:1) mix produced films with higher elasticity than raw kaolin and Ag-Kln (1:2) mix. Incorporation of the silver particles had caused the Ag-Kln (1:2) mix and the Ag-Kln (1:1) mix improved the YM significantly ($p < 0.05$) to higher values, ranging from 63.35 to 115.46 MPa and 63.50 MPa to a high elevation of 376.20 MPa, respectively. As expected, the higher the concentration of Ag-Kln in the composite matrix, the stronger the films produced, consecutively, enhancing the rigidness and elasticity. This is in agreement with the studies from Kanmani and Rhim (2014) when the addition of clay and silver compounds into their gelatin films increased YM value.

Tensile strength (TS) is the resistance of a material to break when tension is applied towards it. Control film possessed the highest TS value compared to kaolin and Ag-Kln films due to the elasticity of gelatin structure which is hard to rupture probably due to the strong peptide bonds presence. The declining effect of the films' intrinsic stiffness was relatively related to the substitution of kaolin particles embedded. This was caused by the surface tension reduction which occurred between gelatin polymer matrix and clay particles. Incomplete dispersion of stacked clay in the polymer network resulted in an irregular structure matrix (Fig. 1c) and affected the film's ability in resisting high stress force. Malleable kaolin clay incorporation in gelatin FFS had separated the clay platelets which left scattered within the solvent as water drives away the platelets apart. In addition, lower TS values with the introduction of silver particles was due to the decrease in inter and intra molecular chain interactions of bio-polymer with the silver compounds (Bang, Shankar, & Rhim, 2019; Shankar & Rhim, 2015). This combination also had resulted in a globular structure of the polymer matrix caused by the silver compounds aggregation, consequence from the hydrophilic gelatin and hydrophobic silver fusion. However, a significant increase was spotted among raw kaolin films and Ag-Kln films. As the concentration increased to 45% for each type of kaolin film, the TS values were also increased significantly ($p < 0.05$).

The increased ability in withstanding high resistant was owing to the silicate's characteristics, such as large surface area (ranging in 750 m^2/g), high aspect ratio (50-1000), and high elastic modulus proportional to the increment of kaolin amount (178 GPa) (Alexandre & Dubois, 2000; Pavlidou & Papaspyrides, 2008; Ray & Bousmina, 2005). Films' TS increased ($p < 0.05$) as silver particles were added into kaolin-gelatin films, possibly due to the interfacial interaction between kaolin and silver in the polymer matrix. The combination of kaolin-gelatin composite film and silver caused the film to become more rigid and stronger. Improvement of this mechanical property can be vividly observed at 45% of both Ag-Kln (1:1) mix and Ag-Kln (1:2) mix films in Table 1. The highest concentration of Ag-Kln film showed a notable value of TS in

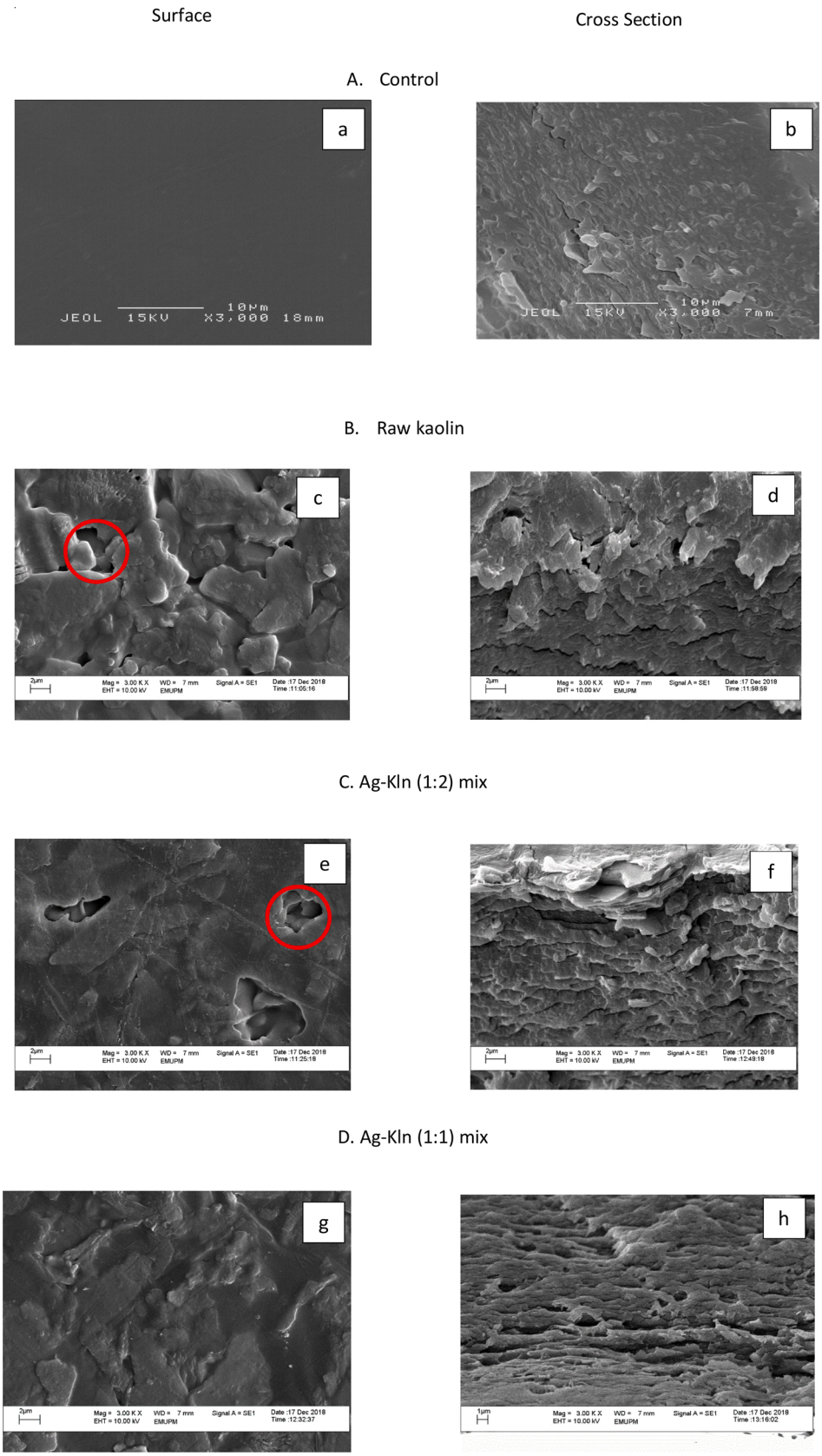

Fig. 1. SEM images of control films and gelatin films incorporated with raw kaolin, Ag-Kln (1:2) mix and Ag-Kln (1:1) mix.

Table 2
UV light transmittance of control gelatin film and gelatin films incorporated with raw kaolin, Ag-Kln (1:2) mix and Ag-Kln (1:1) mix.

Film Samples	Concentration (%)	UV Light Transmittance (%)		Visible Light Transmittance (%)			
		200 nm	280 nm	400 nm	500 nm	600 nm	800 nm
Control	-	65.05 ± 1.35^{Aa}	72.72 ± 0.42^{Aa}	78.34 ± 0.03^{Aa}	81.00 ± 0.12^{Aa}	82.45 ± 0.12^{Aa}	83.98 ± 0.28^{Aa}
Raw Kaolin	15%	22.00 ± 1.10^{Bb}	24.25 ± 0.65^{Bb}	24.00 ± 0.18^{Bb}	27.29 ± 0.10^{Bb}	29.3 ± 0.14^{Bb}	32.60 ± 0.41^{Bb}
	30%	9.52 ± 1.14^{Bc}	10.12 ± 0.94^{Bc}	9.00 ± 1.56^{Bc}	10.96 ± 1.83^{Bc}	12.13 ± 2.01^{Bc}	14.02 ± 2.25^{Bc}
	45%	0.00 ± 0.00^{Bd}	0.23 ± 0.20^{Bd}	0.54 ± 0.19^{Bd}	0.83 ± 0.27^{Bd}	1.02 ± 0.32^{Bd}	1.36 ± 0.46^{Bd}
Ag-Kln (1:2) mix	15%	19.80 ± 3.55^{Bb}	22.69 ± 0.94^{Bb}	22.09 ± 1.91^{Bb}	25.21 ± 2.05^{Bb}	27.07 ± 2.16^{Bb}	30.22 ± 2.41^{Bb}
	30%	9.51 ± 1.88^{Bc}	12.06 ± 1.27^{Bc}	11.66 ± 1.07^{Bc}	14.05 ± 1.23^{Bc}	15.55 ± 1.33^{Bc}	18.12 ± 1.54^{Bc}
	45%	0.15 ± 0.03^{Bd}	0.86 ± 0.52^{Bd}	1.37 ± 0.30^{Bd}	1.77 ± 0.03^{Bd}	1.97 ± 0.07^{Bd}	2.25 ± 0.02^{Bd}
	15%	8.42 ± 0.47^{Cb}	11.32 ± 4.34^{Cb}	10.71 ± 3.29^{Cb}	12.82 ± 3.84^{Cb}	14.01 ± 4.17^{Cb}	16.07 ± 4.92^{Cb}
Ag-Kln (1:1) mix	30%	0.00 ± 0.00^{Cc}	0.72 ± 0.55^{Cc}	1.83 ± 0.60^{Cc}	2.39 ± 0.78^{Cc}	2.68 ± 0.88^{Cc}	3.09 ± 1.04^{Cc}
	45%	0.00 ± 0.00^{Cd}	0.00 ± 0.00^{Cd}	0.07 ± 0.01^{Cd}	0.14 ± 0.10^{Cd}	0.17 ± 0.11^{Cd}	0.18 ± 0.11^{Cd}

Values are given as mean ± standard deviation.
Small letters (a,b,c,d) in the same column indicate significant difference between concentrations ($p < 0.05$).
Capital letters (A,B,C) in the same column indicate significant difference between type of kaolin ($p < 0.05$).

accordance to Yoksan and Chirachanchai (2010) who also obtained a superior increase of TS when a larger amount of silver particle was incorporated. Kaolin inclusion at a low rate could cause an impact on the disruption of the polymer networks, therefore decreased the flexibility of kaolin-gelatin composite films. However, the presence of silver compounds had resulted an intense on the inter- and intra-molecular chain networks (Basumatary et al., 2018). Thus, increased the films' TS.

Elongation at break (EAB) expresses the capability of a material to resist changes of shape without crack formation. However, EAB values were inversely proportional to the type of kaolin and concentration. Table 1 portrays that control film exhibited the highest value and there was no significant effect between control film and raw kaolin film. As the silver compound added into kaolin-gelatin films, a significant ($p < 0.05$) decrease was noted, from 17.18% to 4.32%. An increase in concentration also resulted in a significant decline in EAB value for each type of kaolin film. Generally, the addition of Ag-Kln in gelatin composite films showed a depletion ($p < 0.05$) for EAB indicating the less flexibility of the films (Voon, Bhat, Easa, Liong, & Karim, 2012). This was probably attributed to the presence of kaolin clay which restrains the molecular motion of the polymer chains in the matrix.

3.1.4. Scanning Electron Microscopy (SEM)

Images obtained by SEM indicated that control film, as expected had the smoothest and even surface as opposed to the films with kaolin and Ag-Kln addition (Fig. 1a). On the other hand, raw kaolin film was viewed with intercalated sheets and cracks formation. This implies that kaolin incorporation resulted in heterogeneous film. As discussed previously on the increasing of the films' thickness (Table 1), it could also be one of the factors for the rougher films produced when kaolin was introduced in gelatin composite film. Possibly, the protein network was affected by the kaolin particles which disrupted the smoothness of the film's structure. A similar trend of irregular film's structure with kaolin addition was reported by Jafarzadeh et al. (2017). Nevertheless, films' structures were observed with less micro pores when silver particles were added into the FFS which also aided in uniformities of the film (Fig. 1e-h). The pores and cracks formation were marked (circle) in Fig. 1c and e. No detectable separation was to be seen for silver-kaolin (1:1) mix film and the structure became more linear. Ag-Kln (1:1) mix film showed more homogenous surface compared to raw kaolin and Ag-Kln (1:2) mix films, which implied that as silver concentration increased, particles within the films became more compatible with each other. This explained that the surface distribution pattern was affected by the concentration of kaolin clay and silver particles used. Bang et al. (2019) also reported that silver was homogenously dispersed in gelatin-based film, due to silver's high surface to volume ratio and the increase of Ag + content (Shankar & Rhim, 2017) in kaolin. The interaction between Ag-Kln and gelatin showed a uniform distribution and eventually, developed an even surface without agglomeration as shown in Fig. 1g.

3.1.5. Atomic Force Microscopy (AFM)

The atomic force microscopy (AFM) images are shown in Fig. 2. The least roughness value (Rq) of the film was obtained at 0.003 μm for the control film. Root mean roughness of the films (Rq) was calculated and the results were similar to data reported by Alexandre, Lourenço, Bittante, Moraes, and do Amaral Sobral (2016) about montromorillonite clay films that having rougher surface compared to control film. The results supported that kaolinite attributes were the reason for the increasing roughness value of the film which also explained that the accumulation of clay being lodged in the bio-composite film has reached above certain extent (Rhim, 2011). Nonetheless, when silver compound was embedded in the kaolin-gelatin film, the roughness value dropped to 0.109 μm and became more ceaseless which was also considered as a homogenous structure. Roughness value increased when kaolin content elevated up to 45% of incorporation and gradually dropped as silver particles were added. Silver attributes are so divergent, including having a good solubility rate, thus, describing this substance as being highly soluble (Greenwood & Earnshaw, 2012) and easily dispersed in kaolin-gelatin FFS. AFM results were corresponding to previous analysis (SEM) that by adding silver particles in kaolin-gelatin films aided in increasing the cohesiveness of the films' matrix network. Peaks formed were also less as the concentration of Ag-Kln increased.

3.1.6. Ultra-Violet Light Transmission Property

Direct UV light exposure to food products can deteriorate the quality. Ramos et al. (2013) stated that ultra violet (UV) light barrier property is required to protect food as well as to sustain its nutrients and to prevent lipid oxidation. By packing food in low UV light transmittable films, it will also forbid the discolouration of food stuffs. Namely, three zones of UV region have been acknowledged generally; UVC (180–280 nm), UVB (280–320 nm) and UVA (320-400 nm).

Gelatin alone as based in the film was highly transparent without any colour to be observed as protective property. Table 2 shows that the control film had the highest absorbance measurement for all wavelengths and made a significant reduction when kaolin was incorporated. Therefore, by adding kaolin clay, the UV barrier was increased. Raw kaolin films' absorbance values reduced ($p < 0.05$) from 32.60% to 1.36% for the highest visible light wavelength (800 nm) inversed proportional to the concentration. Gelatin films with Ag-Kln also displayed excellent optical properties, mainly as UV light barriers. For the UVA, as more silver particles been added, there was a significant decrease ($p < 0.05$) until only 1.37% and 0.07% of ultraviolet light transmittance could be pass-through at 45% of Ag-Kln (1:2) mix and Ag-Kln (1:1) mix films, respectively. At 800 nm of wavelength, 45% of Ag-Kln (1:2) mix film showed 2.25% of absorbance, whereas Ag-Kln (1:1) mix film experienced a lower transmission rate, which is 0.18% of absorbance value. The increasing amount of silver particles aided in deterring the UV light transmission.

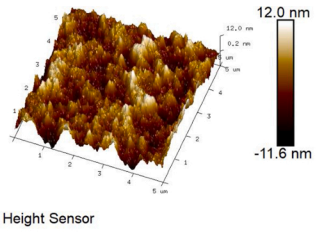

a) Control
Rq: 0.003 µm

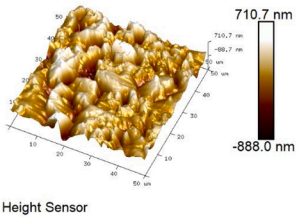

b) 15% Raw Kaolin
Rq: 0.121 µm

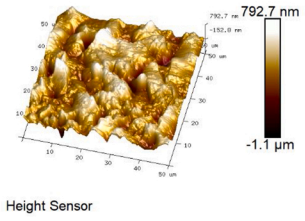

c) 30% Raw Kaolin
Rq: 0.166 µm

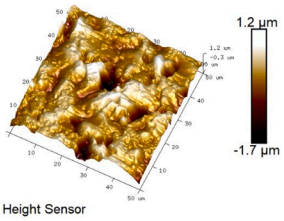

d) 45% Raw Kaolin
Rq: 0.180 µm

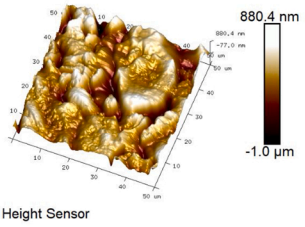

e) 15% of Ag-Kln (1:2) mix
Rq: 0.198 µm

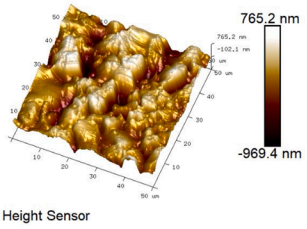

f) 30% of Ag-Kln (1:2) mix
Rq: 0.178 µm

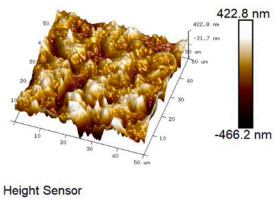

g) 45% of Ag-Kln (1:2) mix
Rq: 0.109 µm

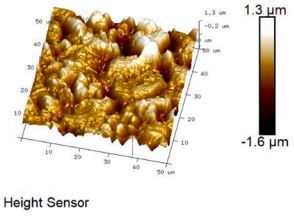

h) 15% of Ag-Kln (1:1) mix
Rq: 0.260 µm

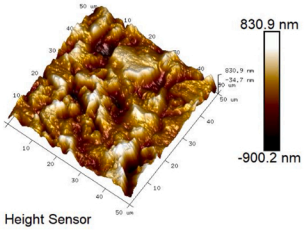

i) 30% of Ag-Kln (1:1) mix
Rq: 0.181 µm

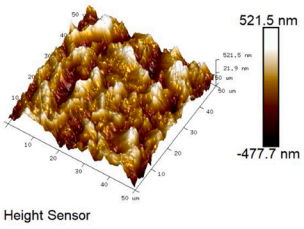

j) 45% of Ag-Kln (1:1) mix
Rq: 0.118 µm

Fig. 2. Atomic force microscopic (AFM) images of control films and gelatin films incorporated with raw kaolin, Ag-Kln (1:2) mix and Ag-Kln (1:1) mix.

Protein-based films have a great amount of aromatic amino acids, such as phenylalanine, tyrosine, and tryptophan that are believed to protect the film from UV light transmission (Arfat, Benjakul, Prodpran, Sumpavapol, & Songtipya, 2014) by absorbing more UV radiation (Ramos et al., 2013). Hence, it helps in protecting the packaged food. Gelatin protein, unluckily, is absent with tryptophan and only has a small amount of phenylalanine and tyrosine (Hafidz, Yaakob, Amin, & Noorfaizan, 2011). Thus, explaining the low barrier capability of gelatin film in blocking the UV transmission at these wavelengths compared to other protein-based films (Sáez-Orviz, Marcet, Weng, Rendueles, & Díaz, 2020). The significant increase in film's UV barrier property was due to the silver compounds reinforcement which successfully hindered the light refraction index caused by the interaction of Ag + ion in bio-based polymers (Kanmani & Rhim, 2014). The UV light transmittance percentages for gelatin-based films incorporated with kaolin and silver particle were significantly lowered than those obtained by Jafarzadeh et al. (2017) when using semolina film with kaolin alone. This phenomenon was probably due to the residues of phenylalanine and tyrosine (Hansen, Jamali, & Hubbuch, 2013) in gelatin component (Huang et al., 2020) and active compounds particle dispersed within the composite film matrix. Consequently, obstructed the light scattering which passed through the polymer (Kanmani & Rhim, 2014). Hence, these results demonstrated that the Ag-Kln compound distribution within gelatin film had provided a protection against the UV passage owing to the films' opaqueness and Ag-Kln aggregation within the film matrix.

3.2. Water Barrier Properties of Films

3.2.1. Water Solubility

The initial mass of the films were lesser than the final mass as the water had been absorbed by the films. A strong hydrogen bond can hold gelatin and water molecule together to increase the diffusivity coefficient, and resulting in an excellent water barrier property (Carvalho, Grosso, & Sobral, 2008). No significant difference was detected for control gelatin film and raw kaolin film. Nonetheless, as more silver particles were incorporated into the films, the solubility rate decreased significantly ($p < 0.05$) (Table 3). This stipulated that the addition of Ag-Kln helped in reducing the water uptake ratio of the films as demonstrated from moisture content (MC) analysis. Water solubility (WS) of raw kaolin composite film initially was 28.40% and it decreased ($p < 0.05$) with the increase of the kaolin clay content down to 20.50%, then it dropped substantially significant to 15.20% when Ag-Kln (1:1) mix was added. The water solubility was affected by the concentration and the type of kaolin used. Nyflött et al. (2017) agreed that clay addition improved polymer's water barrier properties as the platelet layers altered the matrix and formed tortuous paths which made the diffusional channel harder to be penetrated by water molecules. Similar phenomena also have been reported by Rhim (2011) and Casariego et al. (2009). In addition, Ag-Kln in gelatin composite film produced better water retention than having clay incorporated in chitosan-based film (Casariego et al., 2009). This is generally concerning the robust interaction allying the hydroxyl groups and protein-based polymer via hydrogen bonds with large surface area, hence affecting the water solubility property.

It is important to note that the bio-polymer and clay interaction which occurred in the film matrix lowered the availability of hydroxyl and amino groups that can interact with water, thus decreasing the films' water solubility (Rhim, 2011). The reduction in solubility was more intense at 45% of Ag-Kln (1:1) mix film, indicating that the silver particles reinforced decreased the composite films' hygroscopicity, which agrees to the data obtained in WVP (Table 3).

3.2.2. Water Vapour Permeability (WVP)

Sensitive or perishable food products should be protected by packaging materials that can act as a barrier against moisture to prevent spoilage, which will result in longer shelf life. WVP of the gelatin films dropped significantly as kaolin was introduced (Table 3). Silver particles added subsequently reduced the WVP values even more ($p < 0.05$) with 15% for any type of kaolin films showed higher WVP compared to 30% and 45% kaolin films. The hydrogen bonds formed within the polymer matrix had reduced the availability of hydroxyl and amino groups to associate with water (Boughriba, Souissi, Jridi, Li, & Nasri, 2020; Voon et al., 2012), thus, resulted in low WVP.

Table 3
Water solubility, water vapour permeability (WVP), water contact angle and moisture content of control gelatin film and gelatin films incorporated with raw kaolin, Ag-Kln (1:2) mix and Ag-Kln (1:1) mix.

Film Samples	Concentration (%)	Water Solubility (%)	WVP (g/m s Pa) x 10^{-12}	Water Contact Angle (°)	Moisture Content (%)
Control	-	29.10 ± 0.26^{Aa}	1.59 ± 0.09^{Aa}	61.94 ± 1.96^{Bb}	1.91 ± 0.01^{Aa}
Raw Kaolin	15%	28.40 ± 0.26^{Aa}	1.17 ± 0.09^{Bb}	112.80 ± 9.9^{Aa}	1.67 ± 0.26^{Ba}
	30%	22.60 ± 0.46^{Ab}	1.14 ± 0.01^{Bbc}	112.96 ± 3.22^{Aa}	1.06 ± 0.24^{Bb}
	45%	20.50 ± 0.51^{Ab}	1.11 ± 0.02^{Bc}	116.03 ± 3.88^{Aa}	0.74 ± 0.25^{Bc}
Ag-Kln (1:2) mix	15%	16.60 ± 0.26^{Ba}	1.08 ± 0.02^{Cb}	113.33 ± 2.46^{Aa}	1.41 ± 0.04^{Ca}
	30%	10.70 ± 0.27^{Bb}	1.04 ± 0.03^{Cbc}	114.51 ± 3.17^{Aa}	0.92 ± 0.01^{Cb}
	45%	9.10 ± 0.02^{Bb}	1.03 ± 0.02^{Cc}	116.38 ± 0.46^{Aa}	0.46 ± 0.01^{Cc}
Ag-Kln (1:1) mix	15%	15.20 ± 0.27^{Ba}	1.07 ± 0.05^{Cb}	113.87 ± 4.24^{Aa}	0.92 ± 0.01^{Da}
	30%	9.00 ± 0.01^{Bb}	1.05 ± 0.04^{Cbc}	115.31 ± 1.11^{Aa}	0.60 ± 0.25^{Db}
	45%	8.80 ± 0.01^{Bb}	1.02 ± 0.09^{Cc}	116.74 ± 1.44^{Aa}	0.45 ± 0.01^{Dc}

Values are given as mean ± standard deviation.
Small letters (a,b,c) in the same column indicate significant difference between concentrations ($p < 0.05$).
Capital letters (A,B,C,D) in the same column indicate significant difference between type of kaolin ($p < 0.05$).

A gradual decrease in WVP explained that films were improved on the presence of kaolin and silver addition, which limited the interaction with water macromolecules, thus leaving less free hydroxyl groups for water binding (Mbey et al., 2012). The interaction occurred included the rearrangement of protein network and minerals introduction. Kaolin generated an excessive complex path for water diffusion within the polymer matrix. In this way, a natural tetrahedral sheet of silica in kaolin linked through oxygen atoms acts as a natural cross-linker, leading to a more rigid and compact film matrix and improved the films' physical properties. Furthermore, kaolin clay particles are hydrophobic in nature, thus helping in reducing the WVP (Mbey et al., 2012), as supported by contact angle analysis.

3.2.3. Moisture Content

Based on the results in Table 3, MC of the composite films ranged from 1.91% to 0.45%. Control film had the highest value of moisture content and decreased ($p < 0.05$) as kaolin and silver compound was added. In general, the surface structure of normal gelatin film is hydrophilic, yet kaolin and silver compounds had successfully altered the physical properties of gelatin films. Hence, by increasing the concentration of Kln and Ag-Kln, cohesiveness of the films increased, which in turn produced hydrophobic films as supported by WVP.

According to Kanmani and Rhim (2014), moisture content which also could be translated to the total water molecules within the network microstructures of the film is one of the major properties to be counted in for a desirable active packaging material property. Kaolin platelets in the composite film had changed the material's structure arrangement

and behaviour. They interlinked the original hydrophilic chains by embedding at the amino acid branches with the tetrahedral side on the outer part. These altered sequences are less likely to attach with hydroxyl groups, hence, resulting in low moisture content (Gopalakrishnan et al., 2011). The addition of Ag-Kln into gelatin films caused the reduction of the polymer chains interactions, consequently, elevated the hydrophobicity property of the films. Jafarzadeh et al. (2017) also obtained less MC due to kaolin incorporation.

3.2.4. Water Contact Angle

Water contact angle (WCA) which is one of the basic wetting properties was done by measuring the degree of water droplet onto the surface of the films (Table 3). Control film had the lowest value of WCA which was 61.94°, and significantly increased ($p < 0.05$) as kaolin powder was added. Silver incorporation also enhanced the hydrophobicity. Nonetheless, a raised in concentration did not give any notable effects towards all types of kaolin films. Kaolin films' WCA ranged from 112.80° to 116.74° were considered as high value (Rhim, Hong, Park, & Ng, 2006) and concluded that films made from kaolin and addition of silver particles were hydrophobic. Hence, with the presence of silver-kaolin, films' surfaces' cohesiveness level up. These results proposed that by combining gelatin with silver and kaolin, the chemical structure became more rigid, owing to the kaolin tetrahedral sheet and hydrophobic nature of silver (Bang et al., 2019) which made it less accessible to water. WCA degree values were also found to be influenced by the presence of kaolin particles which caused the reduction of polymer-polymer interaction. Kaolin and silver particles had filled in the micro voids in the polymer material, hence, enhanced the net water barrier effect. Eventually, film with a lower surface tension was developed (Yoksan & Chirachanchai, 2010). The findings supported the previous WVP results, and to sum up, data shown were superior in contrast to the information obtained for montmorillonite clay in agar-gellan gum film which is high in swelling capacity (Lee, Rukmanikrishnan, & Lee, 2019).

3.3. Antimicrobial Activity

3.3.1. Disc Diffusion Method (DDM)

The antibacterial activities of Ag-Kln in gelatin composite films were tested against Gram-positive and Gram-negative bacteria; four types of isolated bacteria were included, namely *Staphylococcus aureus (S. aureus), Listeria monocytogenes (L. monocytogenes), Salmonella typhimurium (S. typhimurium), and Escherichia coli (E. coli)*. As stated in studies, these bacteria are generally familiar food pathogens that are most likely to be found in food which causes food spoilage (Girdthep et al., 2014). Table 4 displays the inhibition zones of gelatin control film and three different types of kaolin films. Control films clearly showed no inhibitory zone.

Raw kaolin on the other hand, which acts as a carrier for antimicrobial agent showed the lowest inhibitory activities among kaolin films (7.30 mm to 8.00 mm), close to the data reported by Kanmani and Rhim (2014). According to Priyadarshini, Gopinath, Priyadharsshini, MubarakAli, and Velusamy (2013), Gram-positive bacteria possess three-dimensional thick peptidoglycans (PG; ~20-80 nm) layer composing of short peptides of polysaccharide chains and resulting in a multiplex structure. This explained why the kaolin clay compound alone hard to invade Gram-positive bacteria at 15% of concentration. In spite of that, a significant difference could be noticed as the concentration increased. Nonetheless, a thin PG layer (~7-8 nm) coats Gram-negative bacteria with the negatively charged outer membrane, thus the bacteria are easier to be penetrated. Xu et al. (2006) had revealed that *S. aureus* was less susceptible compared to *E. coli* against silver composite films and implied that the antibacterial activities could be influenced by both chemical structure and bacterial cell wall structure. When kaolin clay was embedded with silver particles, inhibition zone diameter (IZD) became larger. The IZD for Ag-Kln films regardless of the concentration, ranged from 7.80 to 13.00 mm. *S. aureus* had the remarkable highest IZD when tested by the disc diffusion method (DDM) for all films as supported by research (Jou & Malek, 2016), followed by *L. monocytogenes* with 12.33 mm of IZD. Meanwhile, the inhibition halo for Ag-Kln (1:1) mix films against *E. coli* and *S. typhimurium* also embarked significant increases to 9.70 and 9.00 mm, respectively. The increased silver content in kaolin and its concentration in the film larger the IZD of the films towards bacteria, which also stipulated that the highest antimicrobial activity was at 45% of the concentration in Ag-Kln (1:1) mix film. Bacteria were more susceptible to Ag-Kln composite films due to bacterial contact with ionic silver. Silver-kaolin in gelatin films exhibited a wider IZD than previously reported works (Qin et al., 2019; Zhang & Jiang, 2019) which studied regarding chitosan and silver nanoparticles.

Silver is always known as an antimicrobial agent that could penetrate and disrupt microorganism cell wall. Only a few active compounds in silver particles succeed to react with the bacteria, resulting in inhibiting its growth (Sawai, Doi, Maekawa, Yoshikawa, & Kojima, 2002). Hanim, Malek, and Ibrahim (2016) also stated that silver possesses great antibacterial properties and low toxicity. Feng et al. (2000), in their research, claimed that silver plays a significant role in improving the antimicrobial activity because it acts as the stockpile to the Ag^{+} ions released against a broad spectrum of Gram-negative and Gram-positive bacteria. To sum up, films with Ag-Kln (1:1) mix in the gelatin-based film presented a strong antibacterial activity against food-borne pathogens.

4. Conclusions

Gelatin-based packaging films reinforced with kaolin and silver particles were evaluated. The presence of these silver-kaolin compounds

Table 4
Inhibition zone of control gelatin film and gelatin films incorporated with raw kaolin, Ag-Kln (1:2) mix and Ag-Kln (1:1) mix.

Film Samples	Concentration (%)	Inhibition zone of disk diffusion technique (mm)			
		S. aureus (+)	*L. monocytogenes (+)*	*S. typhimurium (-)*	*E. coli (-)*
Control	-	0.00 ± 0.00^{Dc}	0.00 ± 0.00^{Cc}	0.00 ± 0.00^{Cb}	0.00 ± 0.00^{Db}
Raw Kaolin	15%	0.00 ± 0.00^{CDc}	0.00 ± 0.00^{BCc}	7.00 ± 0.00^{Ba}	7.00 ± 0.00^{Ca}
	30%	7.00 ± 0.00^{CDa}	7.00 ± 0.00^{BCa}	7.00 ± 0.00^{Ba}	7.70 ± 0.58^{Ca}
	45%	7.30 ± 0.29^{CDa}	8.00 ± 0.00^{BCa}	7.70 ± 0.58^{Ba}	7.30 ± 0.58^{Ca}
Ag-Kln (1:2) mix	15%	7.80 ± 0.29^{Bb}	8.10 ± 0.66^{Ab}	8.00 ± 0.00^{Aa}	8.20 ± 0.29^{Ba}
	30%	7.30 ± 0.58^{Ba}	8.70 ± 1.16^{Aa}	8.70 ± 0.58^{Aa}	7.70 ± 0.58^{Ba}
	45%	9.30 ± 1.00^{Ba}	9.70 ± 0.58^{Aa}	8.00 ± 1.00^{Aa}	8.50 ± 0.50^{Ba}
Ag-Kln (1:1) mix	15%	8.00 ± 1.00^{Ab}	9.00 ± 1.00^{Ab}	8.30 ± 0.58^{Aa}	8.70 ± 0.20^{Aa}
	30%	11.00 ± 1.73^{Aa}	10.33 ± 1.53^{Aa}	9.00 ± 0.00^{Aa}	9.10 ± 0.12^{Aa}
	45%	13.00 ± 1.00^{Aa}	12.33 ± 2.52^{Aa}	9.00 ± 1.00^{Aa}	9.70 ± 0.58^{Aa}

Values are given as mean ± standard deviation.
Small letters (a,b,c) in the same column indicate significant difference between concentrations ($p < 0.05$).
Capital letters (A,B,C,D) in the same column indicate significant difference between type of kaolin ($p < 0.05$).

had influenced the optical and ultra-violet light transmission. The increase in the concentration of kaolin and silver particles remarkably affected the water barrier properties as supported by the WVP and WCA. On the other hand, AFM and SEM analyses proved that Ag-Kln (1:1) mix films produced better morphology surfaces and structures. Additionally, Ag-Kln films were profoundly inhibited the antimicrobial activity against both Gram-negative and Gram-positive bacteria (*E. coli, S. aureus, L. monocytogenes* and *S. typhimurium)*. Despite of no Ag, films with Kln also had halo of inhibition which explained that Kln particles had the potential to inhibit the bacteria growth. In general, gelatin films with kaolin clay and silver particles demonstrated better functional properties with good compatibility and are recommended for further study as active food packaging materials.

Declaration of Competing Interest

The authors report no declarations of interest.

Acknowledgement

The authors would like to gratefully thank Universiti Putra Malaysia (UPM) for the financial and technical support.

References

Abedinia, A., Ariffin, F., Huda, N., & Nafchi, A. M. (2018). Preparation and characterization of a novel biocomposite based on duck feet gelatin as alternative to bovine gelatin. *International Journal of Biological Macromolecules, 109*, 855–862.

Austin, A. (2007). *The Craft of Silversmithing: Techniques, Projects, Inspiration*. United States: Sterling Publishing Company, Inc.. p. 43. ISBN 978-1-60059-131-0.

Alexandre, E. M. C., Lourenço, R. V., Bittante, A. M. Q. B., Moraes, I. C. F., & do Amaral Sobral, P. J. (2016). Gelatin-based films reinforced with montmorillonite and activated with nanoemulsion of ginger essential oil for food packaging applications. *Food Packaging and Shelf Life, 10*, 87–96.

Alexandre, M., & Dubois, P. (2000). Polymer-layered silicate nanocomposites: preparation, properties and uses of a new class of materials. *Materials Science and Engineering: R: Reports, 28*(1-2), 1–63.

Al-Hassan, A. A., & Norziah, M. H. (2012). Starch–gelatin edible films: Water vapor permeability and mechanical properties as affected by plasticizers. *Food Hydrocolloids, 26*(1), 108–117.

Arfat, Y. A., Benjakul, S., Prodpran, T., Sumpavapol, P., & Songtipya, P. (2014). Properties and antimicrobial activity of fish protein isolate/fish skin gelatin film containing basil leaf essential oil and zinc oxide nanoparticles. *Food Hydrocolloids, 41*, 265–273.

Atarés, L., Bonilla, J., & Chiralt, A. (2010). Characterization of sodium caseinate-based edible films incorporated with cinnamon or ginger essential oils. *Journal of Food Engineering, 100*(4), 678–687.

Bang, Y. J., Shankar, S., & Rhim, J. W. (2019). In situ synthesis of multi-functional gelatin/resorcinol/silver nanoparticles composite films. *Food Packaging and Shelf Life, 22*, Article 100399.

Basumatary, K., Daimary, P., Das, S. K., Thapa, M., Singh, M., Mukherjee, A., et al. (2018). Lagerstroemia speciosa fruit-mediated synthesis of silver nanoparticles and its application as filler in agar based nanocomposite films for antimicrobial food packaging. *Food Packaging and Shelf Life, 17*, 99–106.

Bauer, A. W. (1966). Antibiotic susceptibility testing by a standardized single disc method. *Am J Clin Pathol, 45*, 149–158.

Bergaya, F. B. K. G., & Lagaly, G. (2013). General introduction: clays, clay minerals, and clay science. In *Developments in Clay Science* (Vol. 5, pp. 1–19). Netherlands: Elsevier.

Boughriba, S., Souissi, N., Jridi, M., Li, S., & Nasri, M. (2020). Thermal, mechanical and microstructural characterization and antioxidant potential of Rhinobatos cemiculus gelatin films supplemented by titanium dioxide doped silver nanoparticles. *Food Hydrocolloids, 103*, Article 105695.

Carvalho, R. A. D., Grosso, C. R. F., & Sobral, P. J. D. A. (2008). Effect of chemical treatment on the mechanical properties, water vapour permeability and sorption isotherms of gelatin-based films. *Packaging Technology and Science: An International Journal, 21*(3), 165–169.

Casariego, A. B. W. S., Souza, B. W. S., Cerqueira, M. A., Teixeira, J. A., Cruz, L., Díaz, R., et al. (2009). Chitosan/clay films' properties as affected by biopolymer and clay micro/nanoparticles' concentrations. *Food Hydrocolloids, 23*(7), 1895–1902.

Cheng, H., Ye, F., Chang, J., & Wu, S. (2019). In situ synthesis and thermal shock resistance of a cordierite-mullite composite for solar thermal storage. *International Journal of Applied Ceramic Technology, 16*(2), 772–780.

Christidis, G. E. (2013). Assessment of industrial clays. In *Developments in Clay Science* (Vol. 5, pp. 425–449). Netherlands: Elsevier.

Córdoba, L. J. P., & Sobral, P. J. (2017). Physical and antioxidant properties of films based on gelatin, gelatin-chitosan or gelatin-sodium caseinate blends loaded with nanoemulsified active compounds. *Journal of Food Engineering, 213*, 47–53.

EFSA Panel on food contact materials, enzymes, flavourings and processing aids (CEF). (2011). Scientific Opinion on the safety evaluation of the substance, silver zeolite A (silver zinc sodium ammonium alumino silicate), silver content 2–5%, for use in food contact materials. *EFSA Journal, 9*(2), 1999.

Feng, Q. L., Wu, J., Chen, G. Q., Cui, F. Z., Kim, T. N., & Kim, J. O. (2000). A mechanistic study of the antibacterial effect of silver ions on Escherichia coli and Staphylococcus aureus. *Journal of Biomedical Materials Research, 52*(4), 662–668.

Food and Drug Administration. (2002). *Code of federal regulations, Title 21-food and drugs, chapter I-food and drug administration, department of health and human services, subchapter B-food for human consumption, part 101-food labeling, subpart A-general provisions, sec. 101.12 reference amounts customarily consumed per eating occasion*. Washington, DC: US Government Printing Office. Last retrieved on 2019.

Garrido, T., Leceta, I., de la Caba, K., & Guerrero, P. (2018). Chicken feathers as a natural source of sulphur to develop sustainable protein films with enhanced properties. *International Journal of Biological Macromolecules, 106*, 523–531.

Ghaderi, J., Hosseini, S. F., Keyvani, N., & Gómez-Guillén, M. C. (2019). Polymer blending effects on the physicochemical and structural features of the chitosan/poly (vinyl alcohol)/fish gelatin ternary biodegradable films. *Food Hydrocolloids, 95*, 122–132.

Girdthep, S., Worajittiphon, P., Molloy, R., Lumyong, S., Leejarkpai, T., & Punyodom, W. (2014). Biodegradable nanocomposite blown films based on poly (lactic acid) containing silver-loaded kaolinite: A route to controlling moisture barrier property and silver ion release with a prediction of extended shelf life of dried longan. *Polymer, 55*(26), 6776–6788.

Gómez-Estaca, J., De Lacey, A. L., López-Caballero, M. E., Gómez-Guillén, M. C., & Montero, P. (2010). Biodegradable gelatin–chitosan films incorporated with essential oils as antimicrobial agents for fish preservation. *Food Microbiology, 27*(7), 889–896.

Gopalakrishnan, K., Birgisson, B., Taylor, P., & Attoh-Okine, N. O. (Eds.). (2011). *Nanotechnology in civil infrastructure: a paradigm shift*. Germany: Springer Science & Business Media (Chapter 6).

Greenwood, N. N., & Earnshaw, A. (2012). *Chemistry of the Elements* (2nd ed.). United Kingdom: Elsevier (Chapter 28).

Hafidz, R. M. R. N., Yaakob, C. M., Amin, I., & Noorfaizan, A. (2011). Chemical and functional properties of bovine and porcine skin gelatin. *International Food Research Journal, 18*(2011), 813–817.

Hanim, S. A. M., Malek, N. A. N. N., & Ibrahim, Z. (2016). Amine-functionalized, silver-exchanged zeolite NaY: preparation, characterization and antibacterial activity. *Applied Surface Science, 360*, 121–130.

Hansen, S. K., Jamali, B., & Hubbuch, J. (2013). Selective high throughput protein quantification based on UV absorption spectra. *Biotechnology and Bioengineering, 110*(2), 448–460.

Hosseini, S. F., & Gómez-Guillén, M. C. (2018). A state-of-the-art review on the elaboration of fish gelatin as bioactive packaging: Special emphasis on nanotechnology-based approaches. *Trends in Food Science & Technology, 79*, 125–135.

Hu, C., Wu, J., Xu, X., & Chen, P. (2018). Investigating the effect of andalusite on mechanical strength and thermal shock resistance of cordierite-spodumene composite ceramics. *Ceramics International, 44*(3), 3240–3247.

Huang, T., Fang, Z., Zhao, H., Xu, D., Yang, W., Yu, W., et al. (2020). Physical properties and release kinetics of electron beam irradiated fish gelatin films with antioxidants of bamboo leaves. *Food Bioscience*, Article 100597.

Jafarzadeh, S., Alias, A. K., Ariffin, F., Mahmud, S., & Najafi, A. (2016). Preparation and characterization of bionanocomposite films reinforced with nano kaolin. *Journal of Food Science and Technology, 53*(2), 1111–1119.

Jafarzadeh, S., Ariffin, F., Mahmud, S., Alias, A. K., Hosseini, S. F., & Ahmad, M. (2017). Improving the physical and protective functions of semolina films by embedding a blend nanofillers (ZnO-nr and nano-kaolin). *Food Packaging and Shelf Life, 12*, 66–75.

Jou, S. K., & Malek, N. A. N. N. (2016). Characterization and antibacterial activity of chlorhexidine loaded silver-kaolinite. *Applied Clay Science, 127*, 1–9.

Jridi, M., Boughriba, S., Abdelhedi, O., Nciri, H., Nasri, R., Kchaou, H., et al. (2019). Investigation of physicochemical and antioxidant properties of gelatin edible film mixed with blood orange (*Citrus sinensis*) peel extract. *Food Packaging and Shelf Life, 21*, Article 100342.

Kam, W. Y. J., Mirhosseini, H., Abas, F., Hussain, N., Hedayatnia, S., & Chong, H. L. F. (2018). Antioxidant activity enhancement of biodegradable film as active packaging utilizing crude extract from durian leaf waste. *Food Control, 90*, 66–72.

Kanmani, P., & Rhim, J. W. (2014). Physical, mechanical and antimicrobial properties of gelatin based active nanocomposite films containing AgNPs and nanoclay. *Food Hydrocolloids, 35*, 644–652.

Kavoosi, G., Rahmatollahi, A., Dadfar, S. M. M., & Purfard, A. M. (2014). Effects of essential oil on the water binding capacity, physico-mechanical properties, antioxidant and antibacterial activity of gelatin films. *LWT-Food Science and Technology, 57*(2), 556–561.

Kumar, P. V., Pammi, S. V. N., Kollu, P., Satyanarayana, K. V. V., & Shameem, U. (2014). Green synthesis and characterization of silver nanoparticles using Boerhaavia diffusa plant extract and their anti bacterial activity. *Industrial Crops and Products, 52*, 562–566.

Lee, H., Rukmanikrishnan, B., & Lee, J. (2019). Rheological, morphological, mechanical, and water-barrier properties of agar/gellan gum/montmorillonite clay composite films. *International Journal of Biological Macromolecules, 141*, 538–544.

Lee, S. Y., & Kim, S. J. (2002). Adsorption of naphthalene by HDTMA modified kaolinite and halloysite. *Applied Clay Science, 22*(1-2), 55–63.

Li, X., Yang, X., Deng, H., Guo, Y., & Xue, J. (2020). Gelatin films incorporated with thymol nanoemulsions: Physical properties and antimicrobial activities. *International Journal of Biological Macromolecules, 150*, 161–168.

Liu, C., Huang, J., Zheng, X., Liu, S., Lu, K., Tang, K., et al. (2020). Heat sealable soluble soybean polysaccharide/gelatin blend edible films for food packaging applications. *Food Packaging and Shelf Life, 24*, Article 100485.

Ma, X., & Bruckard, W. J. (2010). The effect of pH and ionic strength on starch–kaolinite interactions. *International Journal of Mineral Processing, 94*(3-4), 111–114.

Maisanaba, S., Pichardo, S., Puerto, M., Gutiérrez-Praena, D., Cameán, A. M., & Jos, A. (2015). Toxicological evaluation of clay minerals and derived nanocomposites: a review. *Environmental Research, 138*, 233–254.

Maryam Adilah, Z. A., Jamilah, B., & Nur Hanani, Z. A. (2018). Functional and antioxidant properties of protein-based films incorporated with mango kernel extract for active packaging. *Food Hydrocolloids, 74*, 207–218.

Mbey, J. A., Hoppe, S., & Thomas, F. (2012). Cassava starch–kaolinite composite film. Effect of clay content and clay modification on film properties. *Carbohydrate Polymers, 88*(1), 213–222.

Mecif, A., Soro, J., Harabi, A., & Bonnet, J. P. (2010). Preparation of Mullite-and Zircon-Based Ceramics Using Kaolinite and Zirconium Oxide: A Sintering Study. *Journal of the American Ceramic Society, 93*(5), 1306–1312.

Murray, H. H. (2000). Traditional and new applications for kaolin, smectite, and palygorskite: a general overview. *Applied Clay Science, 17*(5-6), 207–221.

Nyflött, Å., Meriçer, Ç., Minelli, M., Moons, E., Järnström, L., Lestelius, M., et al. (2017). The influence of moisture content on the polymer structure of polyvinyl alcohol in dispersion barrier coatings and its effect on the mass transport of oxygen. *Journal of Coatings Technology and Research, 14*(6), 1345–1355.

Odeniyi, M. A., Okumah, V. C., Adebayo-Tayo, B. C., & Odeniyi, O. A. (2020). Green synthesis and cream formulations of silver nanoparticles of Nauclea latifolia (African peach) fruit extracts and evaluation of antimicrobial and antioxidant activities. *Sustainable Chemistry and Pharmacy, 15*, Article 100197.

Okada, K., Yoshizaki, H., Kameshima, Y., Nakajima, A., & MacKenzie, K. J. D. (2010). Porous properties of mesoporous silicas from two silica sources (acid-leached kaolinite and Si-alkoxide). *Journal of Porous Materials, 17*(1), 19.

Pavlidou, S., & Papaspyrides, C. D. (2008). A review on polymer–layered silicate nanocomposites. *Progress in Polymer Science, 33*(12), 1119–1198.

Ponce, A. G., Roura, S. I., del Valle, C. E., & Moreira, M. R. (2008). Antimicrobial and antioxidant activities of edible coatings enriched with natural plant extracts: in vitro and in vivo studies. *Postharvest Biology and Technology, 49*(2), 294–300.

Priyadarshini, S., Gopinath, V., Priyadharsshini, N. M., MubarakAli, D., & Velusamy, P. (2013). Synthesis of anisotropic silver nanoparticles using novel strain, Bacillus flexus and its biomedical application. *Colloids and Surfaces B: Biointerfaces, 102*, 232–237.

Qin, Y., Liu, Y., Yuan, L., Yong, H., & Liu, J. (2019). Preparation and characterization of antioxidant, antimicrobial and pH-sensitive films based on chitosan, silver nanoparticles and purple corn extract. *Food Hydrocolloids, 96*, 102–111.

Ramos, Ó. L., Reinas, I., Silva, S. I., Fernandes, J. C., Cerqueira, M. A., Pereira, R. N., et al. (2013). Effect of whey protein purity and glycerol content upon physical properties of edible films manufactured therefrom. *Food Hydrocolloids, 30*(1), 110–122.

Rao, T. N., Babji, P., Ahmad, N., Khan, R. A., Hassan, I., Shahzad, S. A., et al. (2019). Green synthesis and structural classification of Acacia nilotica mediated-silver doped titanium oxide (Ag/TiO_2) spherical nanoparticles: Assessment of its antimicrobial and anticancer activity. *Saudi Journal of Biological Sciences, 26*(7), 1385–1391.

Ray, S. S., & Bousmina, M. (2005). Biodegradable polymers and their layered silicate nanocomposites: in greening the 21st century materials world. *Progress in Materials Science, 50*(8), 962–1079.

Rhim, J. W. (2011). Effect of clay contents on mechanical and water vapor barrier properties of agar-based nanocomposite films. *Carbohydrate Polymers, 86*(2), 691–699.

Rhim, J. W., Hong, S. I., Park, H. M., & Ng, P. K. (2006). Preparation and characterization of chitosan-based nanocomposite films with antimicrobial activity. *Journal of Agricultural and Food Chemistry, 54*(16), 5814–5822.

Roy, S., Shankar, S., & Rhim, J. W. (2019). Melanin-mediated synthesis of silver nanoparticle and its use for the preparation of carrageenan-based antibacterial films. *Food Hydrocolloids, 88*, 237–246.

Sáez-Orviz, S., Marcet, I., Weng, S., Rendueles, M., & Díaz, M. (2020). PLA nanoparticles loaded with thymol to improve its incorporation into gelatine films. *Journal of Food Engineering, 269*, Article 109751.

Salari, M., Khiabani, M. S., Mokarram, R. R., Ghanbarzadeh, B., & Kafil, H. S. (2018). Development and evaluation of chitosan based active nanocomposite films containing bacterial cellulose nanocrystals and silver nanoparticles. *Food Hydrocolloids, 84*, 414–423.

Satterthwaite, D., McGranahan, G., & Tacoli, C. (2010). Urbanization and its implications for food and farming. *Philosophical Transactions of the Royal Society B: Biological Sciences, 365*(1554), 2809–2820.

Sawai, J., Doi, R., Maekawa, Y., Yoshikawa, T., & Kojima, H. (2002). Indirect conductimetric assay of antibacterial activities. *Journal of Industrial Microbiology and Biotechnology, 29*(5), 296–298.

Shankar, S., & Rhim, J. W. (2015). Amino acid mediated synthesis of silver nanoparticles and preparation of antimicrobial agar/silver nanoparticles composite films. *Carbohydrate Polymers, 130*, 353–363.

Shankar, S., & Rhim, J. W. (2017). Preparation and characterization of agar/lignin/silver nanoparticles composite films with ultraviolet light barrier and antibacterial properties. *Food Hydrocolloids, 71*, 76–84.

Sharma, V. K., Yngard, R. A., & Lin, Y. (2009). Silver nanoparticles: green synthesis and their antimicrobial activities. *Advances in Colloid and Interface Science, 145*(1-2), 83–96.

Slivka, V. (2002). *Mining and treatment of silicate (in Czech)*. Praha: Silikatovy Svaz, 443 pp.

Soradech, S., Nunthanid, J., Limmatvapirat, S., & Luangtana-Anan, M. (2012). An approach for the enhancement of the mechanical properties and film coating efficiency of shellac by the formation of composite films based on shellac and gelatin. *Journal of Food Engineering, 108*(1), 94–102.

Suderman, N., Isa, M. I. N., & Sarbon, N. M. (2018). The effect of plasticizers on the functional properties of biodegradable gelatin-based film: A review. *Food Bioscience, 24*, 111–119.

Tongnuanchan, P., Benjakul, S., Prodpran, T., & Nilsuwan, K. (2015). Emulsion film based on fish skin gelatin and palm oil: Physical, structural and thermal properties. *Food Hydrocolloids, 48*, 248–259.

Voon, H. C., Bhat, R., Easa, A. M., Liong, M. T., & Karim, A. A. (2012). Effect of addition of halloysite nanoclay and SiO 2 nanoparticles on barrier and mechanical properties of bovine gelatin films. *Food and Bioprocess Technology, 5*(5), 1766–1774.

Xu, X., Yang, Q., Wang, Y., Yu, H., Chen, X., & Jing, X. (2006). Biodegradable electrospun poly (L-lactide) fibers containing antibacterial silver nanoparticles. *European Polymer Journal, 42*(9), 2081–2087.

Yang, W., Owczarek, J. S., Fortunati, E., Kozanecki, M., Mazzaglia, A., Balestra, G. M., et al. (2016). Antioxidant and antibacterial lignin nanoparticles in polyvinyl alcohol/chitosan films for active packaging. *Industrial Crops and Products, 94*, 800–811.

Yoksan, R., & Chirachanchai, S. (2010). Silver nanoparticle-loaded chitosan–starch based films: Fabrication and evaluation of tensile, barrier and antimicrobial properties. *Materials Science and Engineering: C, 30*(6), 891–897.

Zhang, W., & Jiang, W. (2019). Antioxidant and antibacterial chitosan film with tea polyphenols-mediated green synthesis silver nanoparticle via a novel one-pot method. *International Journal of Biological Macromolecules*. https://doi.org/10.1016/j.ijbiomac.2019.11.093. in press.